Journal of Visualization, Vol. 10, No. 3 (2007) 247

Portfolio

Compressible Thermal Starting Plume

Rast, M. P.*[1], Mendoza, J.*[2] and Clyne, J.*[2]

*1 Laboratory for Atmospheric and Space Physics, Department of Astrophysical and Planetary Sciences, University of Colorado, Boulder, Colorado USA.
E-mail: mark.rast@lasp.colorado.edu

*2 Computational and Information Systems Laboratory, National Center for Atmospheric Research, Boulder, Colorado USA.

Received 1 February 2007 and Revised 12 April 2007

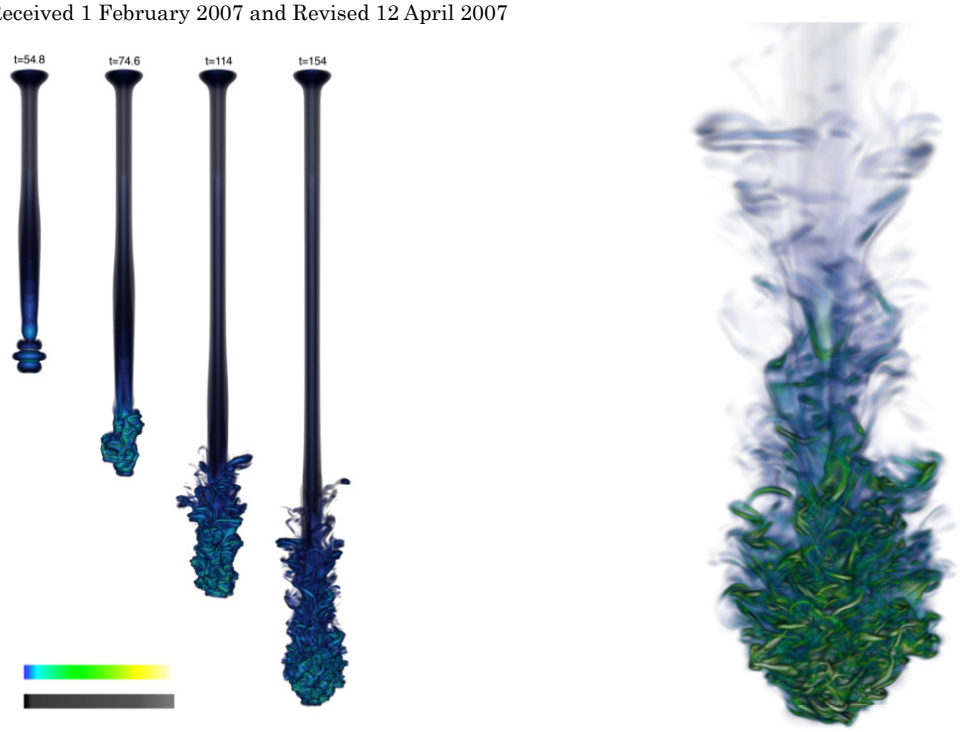

Fig. 1. Numerical simulation of a fully–compressible three–dimensional thermal starting plume descending through an adiabatically stratified domain. Temporal evolution, with time indicated in units of the isothermal sound travel time across the plume diameter at the domain top, on left. On right, a close up of plume head at late time. Images are volume renderings of the flow enstrophy. The color and opacity transfer functions are scaled between zero and the maximum value in the domain at each time step. Opacity bar shows full transparency as black.

The outer one third of the Sun is convectively unstable, driven by heat production in the interior and radiative loss from the photosphere. Surface cooling is non-uniform leading to vigorous new downflow plume formation. These plumes play a crucial role in the dynamics of the flow, interacting to form larger convective scales, and possibly also descend through the entire highly stratified convective layer to play a key role in the transport of heat, momentum, and magnetic field into the overshoot region below. The images above illustrate the enstrophy of a single compressible downflow plume, initiated and maintained by a fixed temperature perturbation imposed on the upper boundary (three – dimensional version of Case E in Rast, M.P., 1998, JFM, 369, 125). The plume is subject to vigorous secondary instability with the successive penetration and disruption of the leading vortex torus by the stem flow from behind. This generates the tangled mass of vortex filaments at the plume head. The computational grid employed was horizontally periodic and highly non – uniform. Only the central one third of the domain is shown after uniform resampling. The images were produced using an open source analysis/visualization package developed at NCAR named VAPoR (www.vapor.ucar.edu).

Journal of Visualization, Vol. 10, No. 3 (2007) 248

Portfolio

Double-Pulse Planar Fuel/Air-Ratio Measurement by Laser-Induced Fluorescence

Scholz, J.*, Wiersbinski, T.* and Beushausen, V.*
* Laser-Laboratorium Goettingen, Hans-Adolf-Krebs-Weg 1, 37077 Goettingen, Germany.
E-mail: Jochen.Scholz@llg-ev.de
Received 19 December 2006 and Revised 30 March 2007

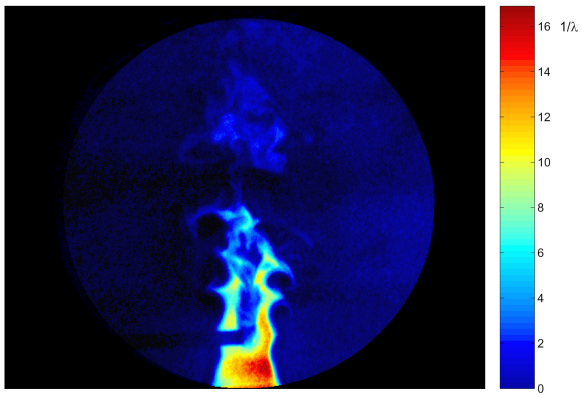

Fig. 1. Map of Fuel/Air distribution.

Fig. 2. Ignitable areas of Fig. 1.

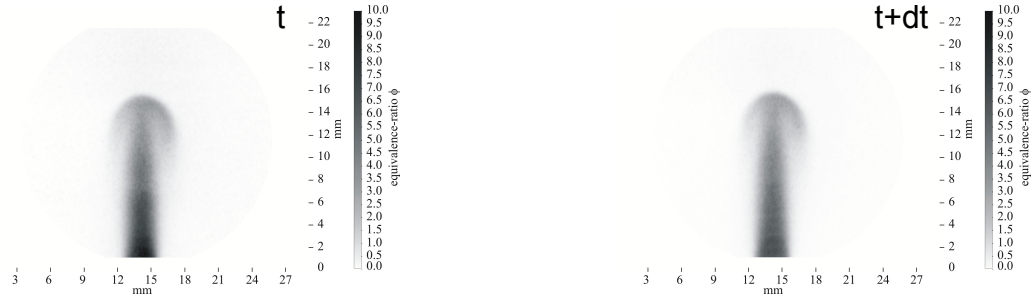

Fig. 3. FARLIF double-pulse image, dt = 2.5 ms.

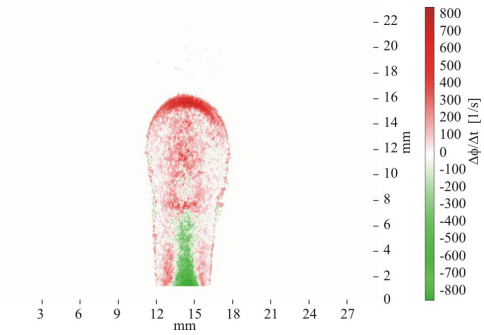

Fig. 4. Temporal derivative of Fig. 3.

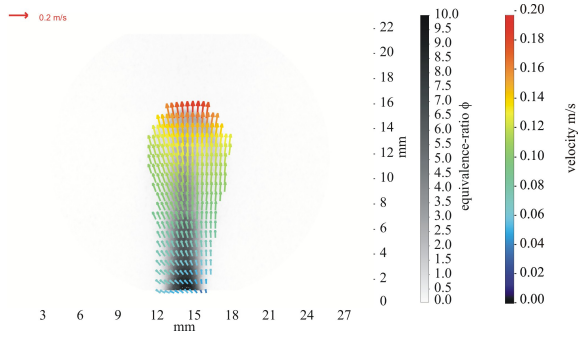

Fig. 5. Fluorescence motion analysis of Fig. 3.

These figures show results of double-pulse fuel/air-ratio measurements by LIF (FARLIF) after fluorescence excitation of a multi-component gasoline (Shell Euro-Super colorless) at 266 nm. This technique may be used to visualize the 2D fuel/air distribution (Fig. 1, mixing of fuel and air in the wake of a cylinder) and to identify ignitable areas (Fig. 2). By using two consecutive images with a small temporal delay (dt), this measurement concept visualizes mixture dynamics (Fig. 3, the change and movement of a rich fuel pulse). This may be used to calculate the temporal derivative of the fuel/air ratio (Fig. 4) and to analyze the motion of mixture structures using optical flow methods (Fig. 5).

Journal of Visualization, Vol. 10, No. 3 (2007) 249

Portfolio

Twin Vortices behind a Flat Plate

Takama, Y.*[1], Suzuki, K.*[2] and Rathakrishnan, E.*[3]
*1 Department of Advanced Energy, Graduate School of Frontier Sciences, The University of Tokyo, 5-1-5 Kashiwanoha, Kashiwa-shi, Chiba, Japan.
E-mail: takama@daedalus.k.u-tokyo.ac.jp
*2 Department of Advanced Energy, Graduate School of Frontier Sciences, The University of Tokyo, 5-1-5 Kashiwanoha, Kashiwa-shi, Chiba, Japan.
*3 Department of Aerospace Engineering, Indian Institute of Technology Kanpur, India.
Received 20 December 2006 and Revised 31 March 2007

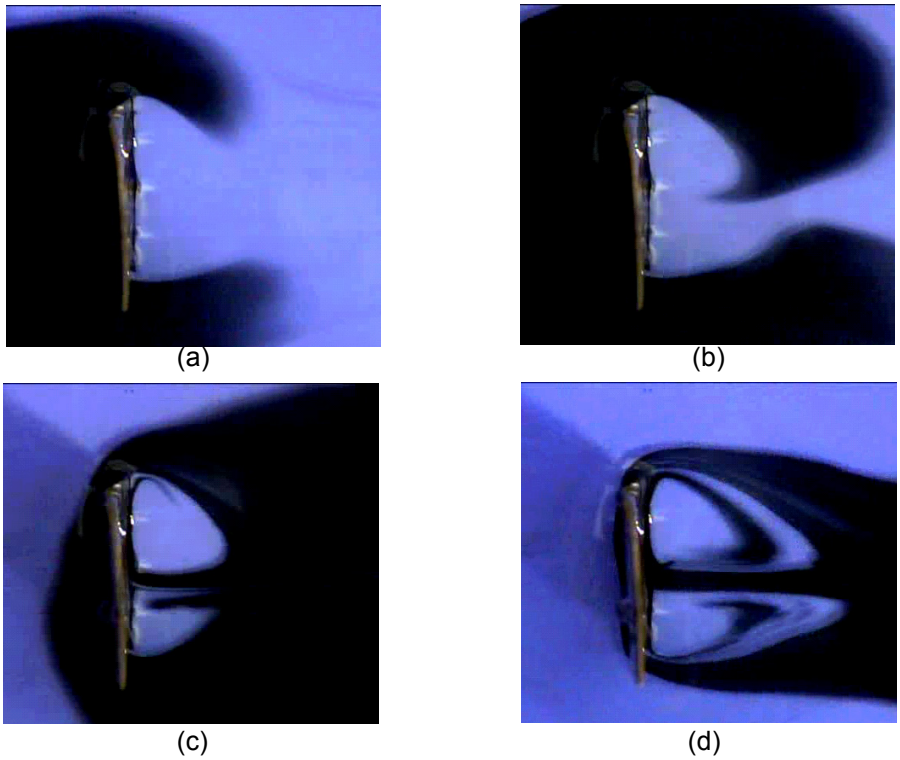

Fig. 1. Twin vortices formation behind a flat plate kept normal to a water stream at Reynolds number 969 (based on plate width).

Water flow visualization with printing-ink was used to capture the evolution and formation of twin vortices behind a flat plate. Uniform flow of water in a rectangular channel was used as the test-section. Twin vortices behind a cylinder are captured at Reynolds number, Re, about 60-140, however for higher Re twin vortices are not formed any more (Ref. 1)*. This is because of the smooth contour of the geometry towards the base. In case of shapes without smooth contour towards base, it may be possible to position the twin vortices at a much higher Re. With this motivation, flow past a flat plate kept normal to the flow was visualized. Flow development was recorded on a video. Four stages of twin vortex formation (Fig. 1) were extracted from the video. The vortices form at Re as high as 969, which is large compared to that of flow over a cylinder. This may be because the sharp turning at the plate edge causes formation of large vortices (Ref. 2)**, leading a higher suction at the base region. This relatively higher suction (compared to a cylinder) makes it possible to hold the twin vortices up to a significantly larger Re.

References : * Houghton, E. L. and Carruthers, N. B., Aerodynamics for Engineering Students, 3rd Edition, (1982), Edward Arnold Ltd., Scotland.
** Lovaraju, P. and Rathakrishnan, E., Subsonic and Transonic Jet Control with Cross-wire, AIAA Journal, 44-11 (2006), 2700-2705.

Journal of Visualization, Vol. 10, No. 3 (2007) 250

Portfolio

Visualization of a Confined Submerged Jet Impinging a Water/Air Free Surface Using DPIV and PLIF

Rivière, N.*[1], Reungoat, D.*[2] and Fauré, J. P.*[1]
*1 CEA Cesta - 12 av Sablieres, 33114 Le Barp Cedex – France.
*2 University of Bordeaux - Lab TREFLE ENSCPB - Pessac – France.
Received 8 January 2007 and Revised 6 April 2007

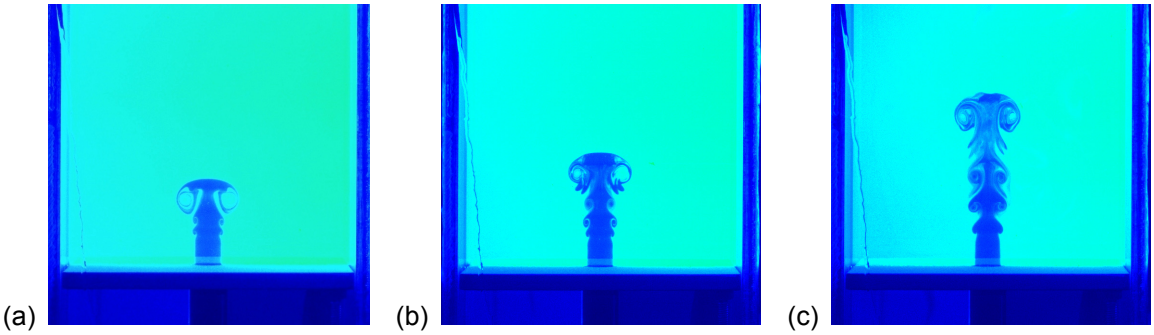

Fig. 1. Concentration fields during starting injection:(a) t_0 + 110 ms, (b) t_0 + 150 ms, (c) t_0 + 220 ms.

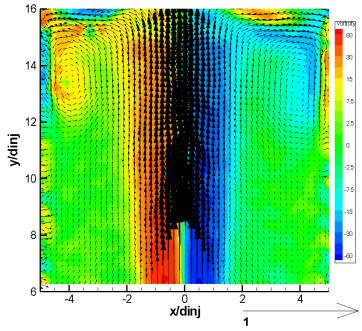

Fig. 2. Mean velocity field under the free surface (dinj = 10 mm, Vinj =1 m/s): vector field and vorticity.

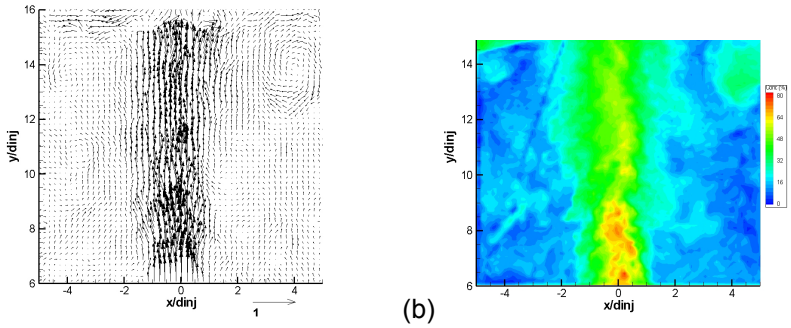

Fig. 3. Simultaneous instantaneous fields: (a) velocity and (b) concentration.

These figures show a turbulent submerged water jet (Re = 10000) entering a rectangular cavity and impinging a water/air free surface, observed thanks to Particle Image Velocimetry (PIV) and Laser-Induced Fluorescence (LIF). Figure 1 displays the starting injection with the development of a vortex ring, the classical ring due to Kelvin-Helmholtz interactions between "pure" water jet and ambient dyed water. Figure 2 shows mean velocity vectors and vorticity field in the upper part of the cavity, with the free jet zone and lateral vortices located between the surface and the vertical walls. Nevertheless these structures do not actually occur simultaneously on both sides of the jet, as it can be seen on instantaneous fields (Fig. 3). The jet is perturbed because of turbulent instabilities and free surface fluctuations. Indeed sequences of instantaneous fields reveal how vortices generated by impingement near the free surface are displaced and sent deeper in the cavity by movements of the interface.

Journal of Visualization, Vol. 10, No. 3 (2007) 251

Portfolio

Influence of the Buoyancy on a Jet in Crossflow

Fraticelli, R.*, David, L.*, Thomas, L.* and Borée, J.*
* Laboratoire d'Études Aérodynamiques, UMR 6909 CNRS Université de Poitiers
ENSMA, Téléport 2 – 1, avenue Clément Ader – BP 40109 – 86961 FUTUROSCOPE
CHASSENEUIL Cedex, France. E-mail: raphael.fraticelli@lea.univ-poitiers.fr
Received 23 February 2007 and Revised 17 April 2007

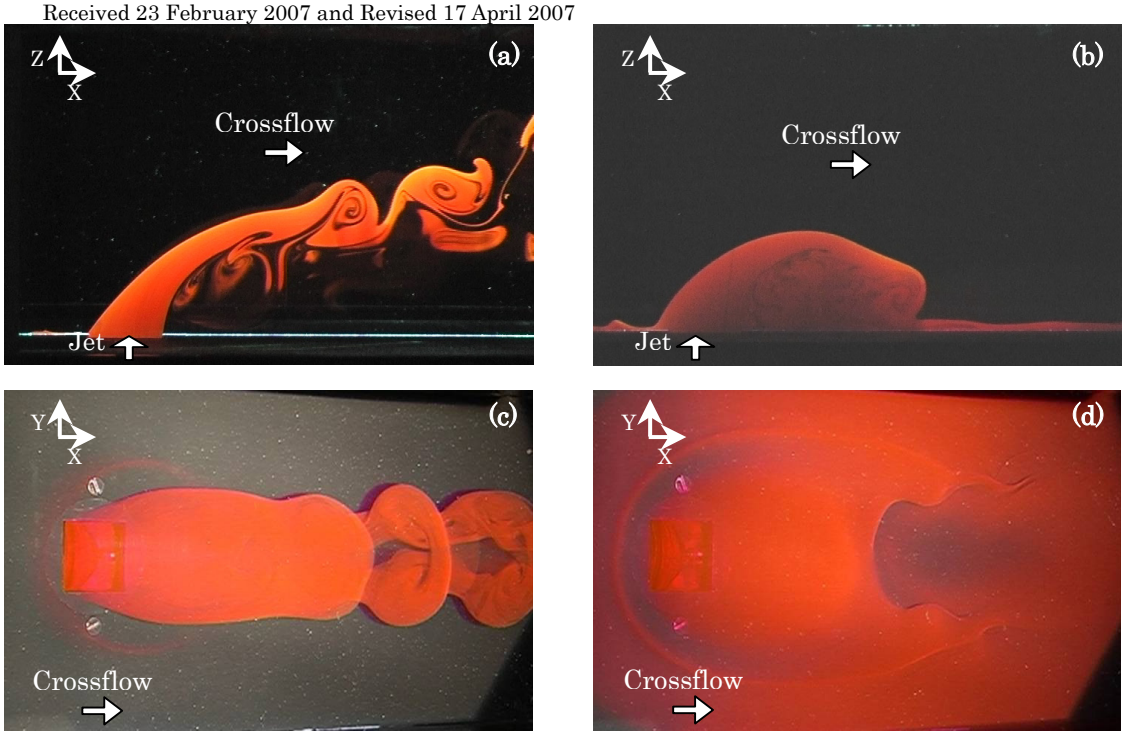

Fig. 1. R = 0.86 – tomographic views (a) and (b) - top views (c) and (d).

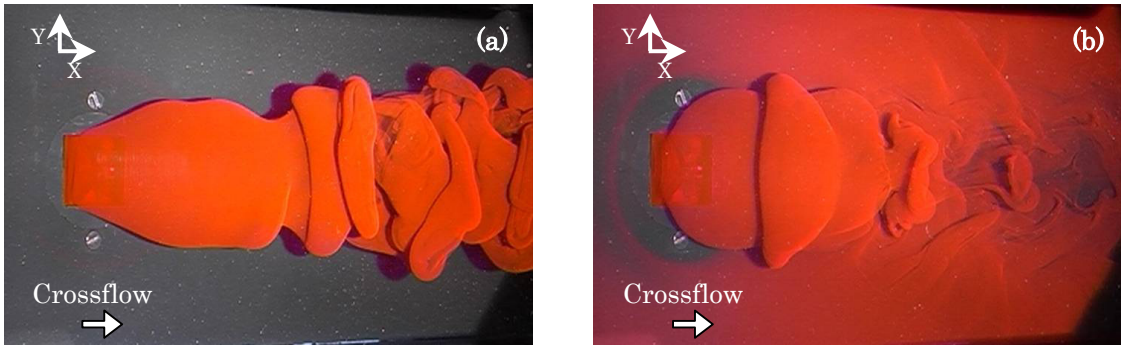

Fig. 2. R = 1.44 – top views (a) and (b).

These figures show colored square jets in crossflow. The Reynolds number is 487, based on the width of the jet orifice. The densimetric Froude numbers (Fr), based on the crossflow velocity and jet orifice, are 1 (right column) and ∞ (left column). R is the momentum ratio of the jet to crossflow. The Atwood number is much lower than 1. The tomographies are made in the symmetrical plan of the flow. The two figures show the influence of densimetric Froude number on the topology of the flow. Several new structures appear in the wake of the negatively buoyant jet (Figs. 1(d) and 2(b)). A transition can be observed, for the Fr = 1 case, between R = 0.86 and 1.44. The two unstationary structures of the R = 0.86 wake are replaced, in the R = 1.44 case, by rings of vortices that fall down on the floor.

References : Fraticelli, R., David, L., Thomas, L. and Borée, J., Influence of the buoyancy on a jet in crossflow, Int. Symposium of Flow Visualisation 12 (Göttingen), (2006-9).

Journal of Visualization, Vol. 10, No. 3 (2007) 252

Portfolio

Whole Flow Field Visualization around a Bullet by Differential Interferometry in Polarized White Light

Desse, J. M.*

* Office National d'Etudes et de Recherches Aérospatiales (ONERA), Centre de Lille, 5, Boulevard Paul Painlevé, 59045 Lille Cedex, France.
E-mail: Jean-Michel.Desse@onera.fr

Received 23 March 2007 and Revised 4 April 2007

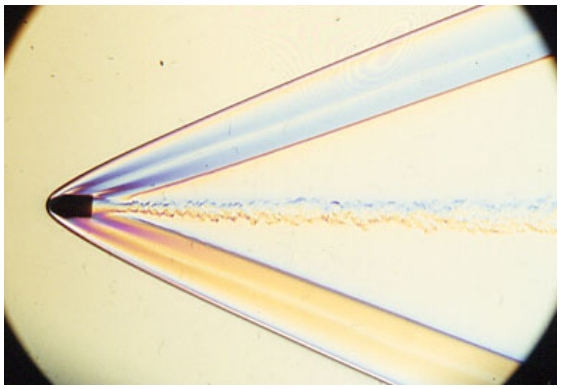

Fig. 1. Wollaston prism angle : 1°.

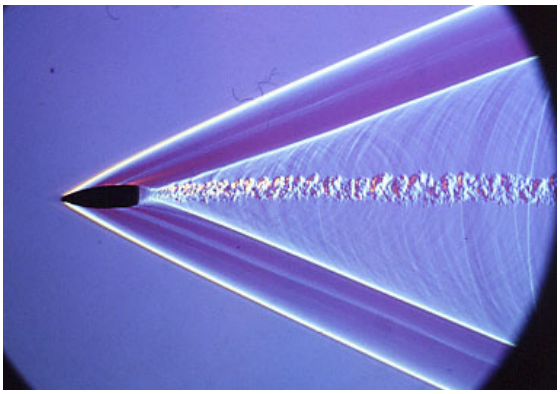

Fig. 2. Visualization of acoustic waves.

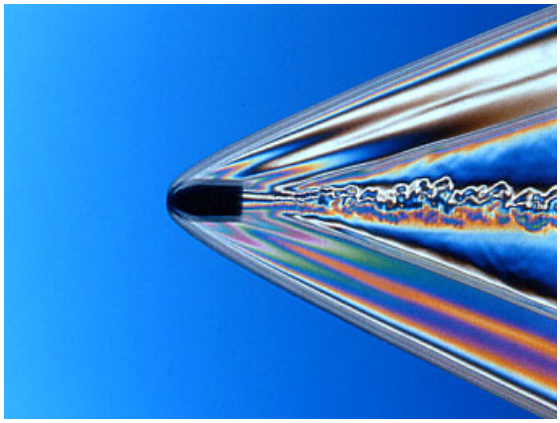

Fig. 3. Wollaston prism angle : 4°.

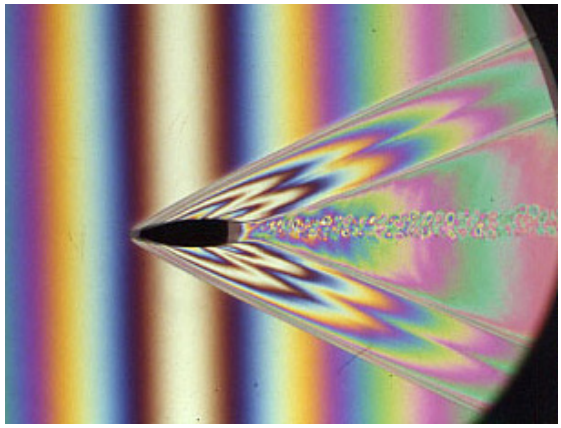

Fig. 4. Finite-fringe mode.

Differential interferometry using a Wollaston prism has been used to visualize the whole flow field around a small bullet (diameters 5.56 mm or 7.62 mm). A double-pass system with the Wollaston prism placed at the curvature center of a spherical mirror is used. The light source is a spark which is triggered when the bullet has reached the centre of the optical test section. The bullet Mach number is 3 and the exposure time of the spark is 300 nanoseconds. Figures 1-3 were taken in so-called infinite-fringe mode just before the firing. Figure 1 shows the gradients perpendicular to the flight path and Fig. 2 the gradients in direction of the bullet trajectory. Moreover, it is possible to see very weak acoustic waves on each side of the wake flow behind the bullet (Fig. 2). In Fig. 3, the Wollaston prism angle is chosen to 4° to strongly increase the sensitivity and the visualized gradients are vertical. This picture shows very well contrasted and saturated colors. Figure 4 shows an interferogram recorded in finite-fringe mode. Here, the difficulty to take this picture lies in the fact that the bullet is just located in the middle of the white fringe. In this configuration, the upper and lower colors of the image situated between the upstream and downstream shock waves are very symmetrical and identical. This particularity gives a wonderful interferogram.